Vol. 52: 343–361, 2023
https://doi.org/10.3354/esr01282

ENDANGERED SPECIES RESEARCH
Endang Species Res

Published December 14

Examining the effect of environmental variability on the viability of endangered Steller sea lions using an integrated population model

Amanda J. Warlick[1,*], Devin S. Johnson[2], Katie L. Sweeney[3], Tom S. Gelatt[3], Sarah J. Converse[4]

[1]School of Aquatic and Fishery Sciences, University of Washington, Seattle, Washington 98195, USA
[2]Pacific Islands Fisheries Science Center, National Marine Fisheries Service, Honolulu, Hawaii 96818, USA
[3]Marine Mammal Laboratory, Alaska Fisheries Science Center, National Marine Fisheries Service, Seattle, Washington 98115, USA
[4]US Geological Survey, Washington Cooperative Fish and Wildlife Research Unit, School of Environmental and Forest Sciences & School of Aquatic and Fishery Sciences, University of Washington, Seattle, Washington 98195, USA

ABSTRACT: Understanding spatio-temporal variability in demography and the influence of environmental conditions offers insight into the factors underlying population dynamics. This is particularly true for species with divergent demographic patterns across large geographic areas. The contrasting abundance trends observed across the range of Steller sea lions *Eumetopias jubatus* have been studied extensively, with research suggesting that the primary drivers of localized population dynamics vary over time and space. We developed a Bayesian integrated population model for the endangered western distinct population segment of Steller sea lions that combines mark-recapture and count data from 2000 to 2021 to estimate demographic rates, abundance trends, and the effects of environmental variability on population growth. Our results highlight subregional demographic differences, including reduced pup survival in the central Aleutian Islands and reduced yearling survival west of Samalga Pass. Range-wide abundance increased by 1.7% yr^{-1} (95% credible interval: 0.14 to 3.4%) over the study period, with a positive annual growth rate of 3.0% (1.1 to 5.1%) yr^{-1} east of Samalga Pass, a negative growth rate of –2.1% (–4.6 to 0.5%) yr^{-1} west of Samalga Pass, and an overall low probability of local extirpation (<2%) in 100 yr even in subregions experiencing continued decline. The effect of environmental variability on population growth varied depending on subpopulation size and vital rates and was strongest in the area of greatest decline. Our model improves upon existing approaches for estimating abundance, accounts for environmental variability within the viability analysis, and can facilitate evaluating the efficacy of conservation actions and progress toward recovery goals.

KEY WORDS: Steller sea lion · Population viability · Integrated population model · Bayesian hierarchical model · Endangered species · Environmental variability

1. INTRODUCTION

Knowledge about spatio-temporal variability in demography can provide valuable insight into the drivers of population dynamics for species that exhibit divergent abundance trends across large geographic areas. This information may be used by resource managers aiming to develop effective conservation strategies for depleted or declining populations. However, estimating vital rates and detecting trends in abundance for depleted top predators with complex life histories and large geographic ranges is challenging, as inferences about broadscale patterns often must be made from spatio-temporally limited

*Corresponding author: amanda.warlick@noaa.gov

Publisher: Inter-Research · www.int-res.com

datasets. Combining multiple data sources within the formal framework of an integrated population model (IPM; Besbeas et al. 2002, Brooks et al. 2004) can improve precision, reduce bias, and facilitate the estimation of parameters not directly informed by data (Schaub et al. 2007, Tavecchia et al. 2009, Abadi et al. 2010). IPMs can also improve the estimation of spatio-temporal variability in demographic parameters, which is fundamental to conducting population viability analyses (PVAs; Beissinger & Westphal 1998) that allow managers to evaluate extinction risk and progress toward recovery goals for populations of conservation concern.

Integrated population modeling is an emerging and evolving tool that has proven useful for examining the population dynamics of long-lived species with complex life histories and behaviors such as cryptic or intermittent breeding (e.g. brown bears *Ursus arctos*, Bled et al. 2017; polar bears *U. maritimus*, Regehr et al. 2018), and for exploring issues of management importance, including the effects of anthropogenic stressors and environmental variability on demography (e.g. Rhodes et al. 2011, Abadi et al. 2017, Cleasby et al. 2017, Pirotta et al. 2022). Using an IPM as the foundation of a PVA can improve demographic estimates and facilitate a full accounting of uncertainty when examining extinction risk or progress toward recovery (Oppel et al. 2014, Saunders et al. 2018). Only a few IPM-based PVAs have been used to evaluate the effects of climate change and management actions on wildlife populations of conservation concern (Saunders et al. 2018), including beluga whales *Delphinapterus leucas* (Mosnier et al. 2015, Warlick et al. 2023), harbor seals *Phoca vitulina* (Boveng et al. 2018), emperor penguins *Aptenodytes forsteri* (Jenouvrier et al. 2019), and Tristan albatross *Diomedea dabbenena* (Oppel et al. 2022).

Steller sea lion (*Eumetopias jubatus*) populations in Alaska declined substantially during the 1970–80s and the species was subsequently listed as threatened under the United States Endangered Species Act (ESA). By the late 1990s, regulations to establish critical habitat and reduce human-caused mortality coincided with the delineation of 2 distinct population segments (DPS) based on differences in genetic composition, diet, and emerging divergent trends in abundance (Loughlin 1997, NMFS 2020). The eastern DPS (ranging from southeast Alaska to northern California) maintained a threatened status and was ultimately delisted in 2013. In contrast, the western DPS (wDPS; ranging from the Gulf of Alaska [GoA] across the Aleutian Islands [AI] into Russia) was relisted as endangered. Divergent abundance trends have subsequently been observed within the wDPS, with stable or increasing abundance to the east of Samalga Pass and declining abundance at rookeries to the west of this dividing line (Fritz & Stinchcomb 2005, Fritz et al. 2016).

In an effort to prevent further declines and promote the recovery of this population, management measures were implemented to address anthropogenic factors that might be hindering recovery, including designating critical habitat (NMFS 1993), monitoring subsistence harvest (NMFS 2008), and regulating commercial fishing activities (NMFS 2001) to reduce bycatch and competition for key prey resources. However, the design and implementation of additional targeted conservation measures remain challenging when the reason(s) for persistent declines are unknown and/or are potentially global in scope (e.g. pollution, climate change). The best available research aimed at understanding the underlying drivers of Steller sea lion population dynamics suggests that demographic factors limiting recovery have likely changed over time and space, and have included lower juvenile survival and fecundity (York 1994, Holmes & York 2003, Holmes et al. 2007), lower breeding-female survival (Maniscalco 2018), and lower pup survival (Warlick et al. 2022). However, these documented demographic differences have not yet been used or estimated in a statistical framework to examine correlations with trends in abundance.

Here we present a PVA for the wDPS of Steller sea lions based on an IPM informed by mark-resight and count survey data to improve upon the existing approach of estimating abundance and to understand the sensitivity of abundance trends and viability to regional demographic differences and environmental variability. This study enhances the information that is available to resource managers by linking localized demography to the regional abundance trends that are the focus of the US ESA downlisting criteria for the wDPS (NMFS 2020). The criteria for downlisting to threatened are 2-fold. First, the overall non-pup abundance trend in the wDPS must be increasing at a specific rate over a 15 yr period. Second, the non-pup trend in 2 adjacent subregions cannot be declining. The first criterion has been met (NMFS 2020), while the second criterion, which relies upon accurate subregional abundance trend estimates, has not been met as of this writing (NMFS 2020), as abundances in subregions west of Samalga Pass continue to decline.

By providing enhanced information about abundance trends and the demographic and environmental drivers of population dynamics, this work can

help managers evaluate progress toward recovery goals, identify knowledge gaps, and inform discussions about the efficacy of existing or future conservation measures. For example, understanding which demographic rates may be limiting population growth could inspire improved specificity of additional management actions or research foci, and provide insight into why existing measures may be insufficient for regions of ongoing conservation concern. Our approach did not necessarily aim to elucidate causal environmental mechanisms driving population dynamics, but does serve as a useful framework for understanding the potential effects of environmental variability or other stressors on population dynamics and viability for populations with divergent abundance trends across a broad region. This work is applicable to other top predators or sentinel species of conservation concern where options for additional conservation measures may be somewhat limited, particularly in light of the challenges of identifying natural and anthropogenic threats, given ongoing and anticipated future climatic changes.

2. METHODS

2.1. Study system

The range of the wDPS of Steller sea lions in Alaska includes rookery and haulout sites along the coastline of the eastern, central, and western GoA and the numerous islands that comprise the eastern, central, and western AI management subregions (Fig. 1). The biological processes driving primary production and ecosystem dynamics in the GoA and across the Aleutian archipelago are shaped by a dividing line at Samalga Pass (170° W; Stabeno et al. 1999, Ladd et al. 2005). Sea lion genetic structure has also been shown to vary between populations to the east and west of this dividing line (O'Corry-Crowe et al. 2006). The shallower passes to the east of Samalga Pass are characterized by a higher diversity of forage fish that supports a more diverse sea lion diet (Sinclair & Zeppelin 2002) compared to the deeper, colder, nutrient-rich passes to the west of Samalga Pass that are dominated by slower-growing forage

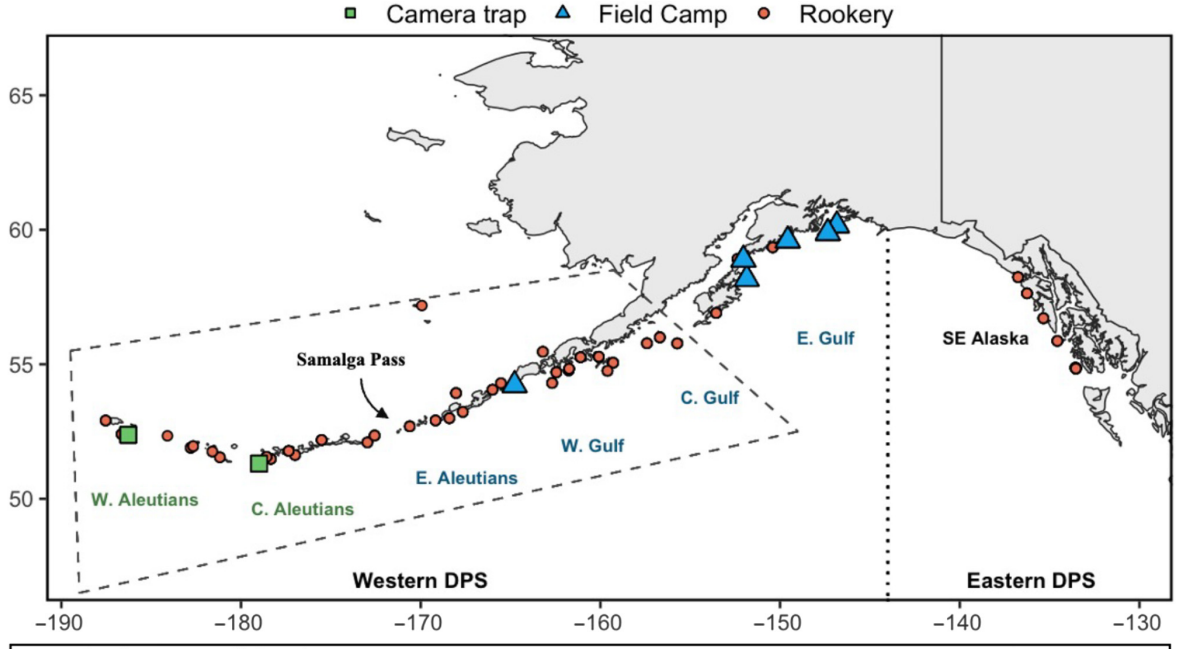

Region	Subregion	2000	2001	2002	2003	2004	2005	2008	2009	2010	2011	2013	2014	2015	2017
Eastern portion of the wDPS range	E. GoA	--	107	--	100	--	80	--	--	--	--	--	--	--	--
	C. GoA	258	--	194	--	185	--	178	--	178	--	--	191	--	--
	E. Aleu	--	175	--	150	--	200	--	188	--	198	--	--	--	86
Western portion of the wDPS range	C. Aleu	--	--	--	--	--	--	--	--	--	--	58	--	51	50
	W. Aleu	--	--	--	--	--	--	--	--	--	54	52	--	50	50

Fig. 1. Steller sea lion field camps in the eastern portion of the range, camera traps in the western portion of the range, and rookeries throughout the western distinct population segment (wDPS) (excluding Russia) and southeast Alaska (eastern DPS, which extends along the US west coast). Dashed rectangle: the spatial extent from which sea surface temperature data were aggregated (46°–58° N, 190°–150° W). Table: the number of branded and released pups in each subregion (none from the western Gulf of Alaska) over the study period

fish (Sinclair et al. 2005, Rand et al. 2019). These regional biophysical characteristics and fine-scale variability affect the foraging conditions experienced by sea lions.

Adult male bulls establish rookery territories starting in May before reproductively mature females arrive to give birth from late May to early July (Pitcher et al. 2001, Kuhn et al. 2017). Throughout the summer, females with pups make short foraging trips that allow them to remain close to the rookery in order to nurse their young and build up energy reserves before going out to sea with their pups for the fall and winter (Raum-Suryan et al. 2002). Females exhibit a high degree of natal site fidelity and begin reproducing between the ages of 3 and 6 yr old (Pitcher & Calkins 1981).

2.2. Data

Two data sources were combined in our model: (1) mark-resight data from sea lions that were hot-branded with individual marks as pups and resighted in 5 subregions of the wDPS range from 2000 to 2018 and (2) model-based pup abundance indices (Johnson & Fritz 2014, Gaos et al. 2021) estimated using raw count survey data from 2000 to 2021 across the wDPS range.

Sea lions were marked using the technique described in Merrick et al. (1996) and Hastings et al. (2009) in accordance with existing permits and Institutional Animal Care and Use committee (IACUC) guidelines and approval. The mark-resight data are conditioned on pup cohorts that were marked late in the summer breeding seasons from 2000 to 2017 at specific rookeries in 5 of the 6 subregions (Fig. 1). Three cohorts (2001, 2003, 2005) were marked at rookeries in the eastern GoA (Seal Rocks, Wooded Is., n = 287), 6 cohorts (2000, 2002, 2004, 2008, 2010, 2014) were marked at rookeries in the central GoA (Marmot and Sugarloaf Is., n = 1184), 6 cohorts (2001, 2003, 2005, 2009, 2011, 2017) were marked in the eastern AI (Ugamak Is., n = 997), 3 cohorts (2013, 2015, 2017) were marked in the central AI (Ulak Is., n = 159), and 4 cohorts (2011, 2013, 2015, 2017) were marked in the western AI (Agattu Is., n = 206). In the eastern portion of the wDPS range (eastern-central GoA, eastern AI), resighting effort occurred May through August during vessel- and land-based surveys, generating a total of approximately 58 360 sighting records of branded females and males. In the western portion of the range (central and western AI), resightings were primarily based on observations generated from remote cameras, amounting to almost 4400 sighting records. Approximately 17% of all marked individuals were resighted outside their natal subregion at some point during the study period.

Count surveys of Steller sea lions throughout Alaska have been conducted since the 1950s, though with more spatio-temporal consistency beginning in the 2000s (Fritz et al. 2016). Surveys generally occurred from late June to early July after most pups are born and when the proportion of animals hauled out is highest (Fritz et al. 2016). Approximately 290 survey sites have been identified across the 6 management subregions. Survey counts were collected from land, ship or skiff, and aerial visual or imagery counts. Visual counts are typically conducted by multiple observers and averaged. Aerial survey images were processed by 2 analysts who independently counted and designated individuals as pups (young of year) and non-pups (juveniles, sub-adult males, adult females, and adult males). As annual surveys are often incomplete because of inclement weather or logistical challenges or accessing remote areas, survey counts from 2000 to 2021 were then modeled using the *mcmc.aggregate* function in the agTrend R package (Johnson & Fritz 2014) to estimate subregional pup abundance indices across all sites (surveyed and unsurveyed) (Sweeney et al. 2022).

To examine the potential effect of environmental variability on sea lion population dynamics, we examined 2 covariates in our analysis: the North Pacific Gyre Oscillation (NPGO) and localized sea surface temperature (SST). The NPGO is an oceanographic index that has been linked to the growth and abundance of various salmon and groundfish species (Di Lorenzo et al. 2008, Kilduff et al. 2015, Ohlberger et al. 2016, Litzow et al. 2018) and was selected as a covariate here because it has been shown to exhibit correlations with sea lion demography (Warlick et al. 2022). Changes in SST coincide with varying localized and basin-scale oceanographic conditions ranging from increased storminess to changes in prey distribution and availability, all of which could affect sea lion survival and reproduction. SST was selected here as a covariate due to the evidence of widespread impacts of the marine heatwave that persisted in the North Pacific from 2015 to 2017 (Arimitsu et al. 2021, Suryan et al. 2021). Monthly data for the NPGO in summer months were obtained from the NOAA National Centers for Environmental Information (NOAA NCEI 2020) and NOAA Physical Sciences Laboratory (NOAA PSL 2020), averaged to create annual values, and *Z*-scored. Though we recognize that environmental conditions and their effects on long-lived top predators vary in complex

ways across the wDPS range, we used a single spatial extent for each covariate across all subregions. Monthly data for SST around the GoA and the AI chain (46°–58° N, 190°–150° W; spatial extent chosen to reflect potential foraging area, though data are sparse) in summer months (June–August) were obtained from the Copernicus Marine Environment Monitoring Service (Martin et al. 2019), averaged over time and space to create a single annual time series, and *Z*-scored. Summer months were chosen for both covariates for simplicity and based on the results of Warlick et al. (2022) that showed the variable effects of the NPGO in different seasons. Though covariate effects were estimated for 2 broad regions independently in Warlick et al. (2022), a single range-wide effect was estimated here, as the subregional sample sizes (particularly in the western portion of the wDPS range) were too small to support independent estimates of covariate effects. We therefore relied on other elements of model structure (e.g. random effects over time and space) to capture spatio-temporal variability in demographic rates across the 6 subregions.

After estimating covariate effects, we used simulations (described in Section 2.4) to examine how the mean and variability in these 2 oceanographic conditions could affect population viability. We randomly generated time series of SST and NPGO values from independent normal distributions for each year based on 8 scenarios that either increased or decreased the mean and/or standard deviation of each covariate for the 100 yr projection period (Table 1).

Table 1. Description of scenarios for generating predicted sea surface temperature and North Pacific Gyre Oscillation for examining the effects of environmental variability on Steller sea lion population dynamics and viability, with mean and standard deviations (SDs) of oceanographic predictors 75% smaller or larger than historical conditions. Percentage change: the average change in population growth rates from the baseline scenario across subregions within the western distinct population segment

Scenario	Mean	SD	Percentage change (%)
1	Historical	Historical	0.000
2		Smaller	0.22
3		Larger	−0.42
4	Low	Smaller	−0.36
5		Historical	−0.57
6		Larger	−0.98
7	High	Smaller	0.75
8		Historical	−0.57
9		Larger	0.12

2.3. Statistical analyses

Our IPM has 2 subcomponent models: a multi-event model (Kendall et al. 2004, Pradel 2005) to estimate demographic rates based on mark-resight data, and a state-space model that uses modeled pup abundance indices based on count survey data to estimate abundance. Multi-event models have been increasingly used to examine vital rates for species with complex life histories (Payo-Payo et al. 2016, Tavecchia et al. 2016, Santidrian Tomillo et al. 2017, Champagnon et al. 2018, Regehr et al. 2018, Himes Boor et al. 2022). As described in Warlick et al. (2022), we use a multi-event model to account for reproductive state uncertainty, as a nursing female may be seen with or without her pup.

2.3.1. Multi-event model

The multi-event model used for the analysis of mark-resight data was similar to that used in Warlick et al. (2022) and is defined by both an ecological process, in which animals transition between true states according to demographic rates, and an observation process, in which individuals are resighted according to detection and state classification probabilities. States were defined by an individual's age, sex, and reproductive state and included pups, yearlings, age-2 individuals, age-3 individuals, age-4 individuals, age-5 individuals, adult females with a pup, adult females without a pup, and adult males (Fig. 2a). We assume that females can have a pup starting at age 4 and must transition into one of the adult female states (with or without pup) by age 6 (no longer a juvenile) conditional on survival. Males are defined as adults at age 6. The state process model,

$$z_{i,t} \mid z_{i,t-1} \sim \text{categorical}(\Omega_{z_{i,t-1},i,t-1}) \quad (1)$$

describes the state z of individual i at occasion t, conditional on the individual's state at the previous occasion, modeled as categorically distributed according to transition array Ω, which is composed of survival ($\phi_{I,t}$) and, for some transitions, pupping probability ($\psi_{I,t}$). We estimate survival for each sex and age, and pupping probabilities describe transitions between states for reproductively active females. Specifically, first-time pupping probability for 4–6 yr old females, $\psi_{3\text{-B:}5\text{-B}}$, describes the probability of pregnancy at ages 3–5 resulting in pupping at ages 4–6. Pupping probability for repeat breeders, $\psi_{\text{B-B}}$, describes the probability that an established breeder has a pup in successive years. Pupping probability for non-breed-

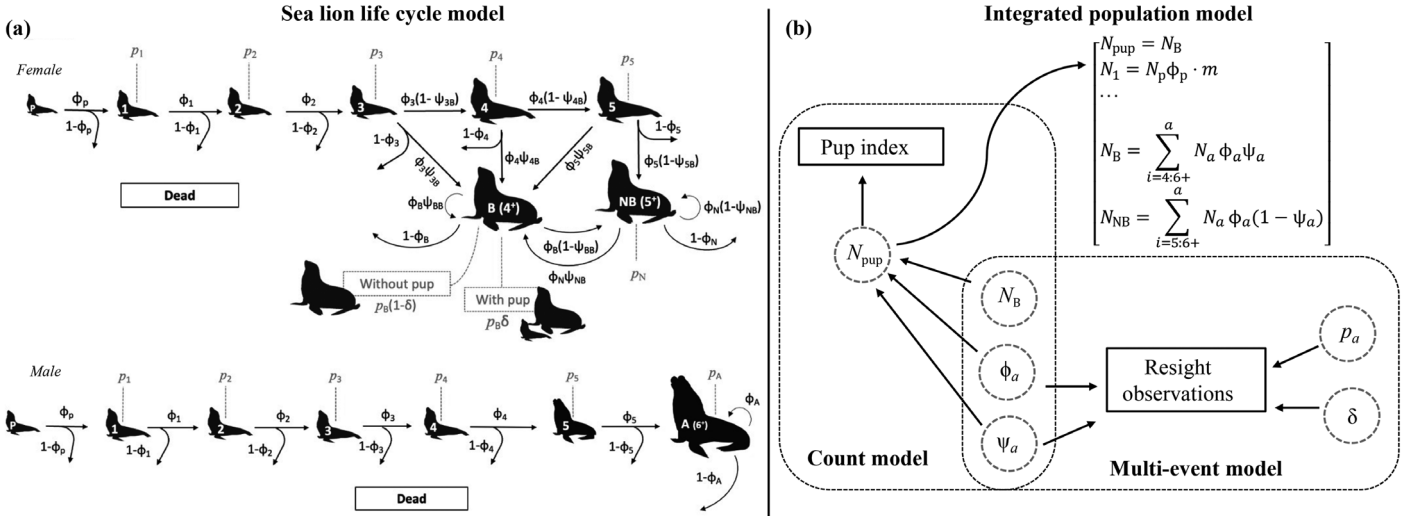

Fig. 2. (a) Life cycle model (reproduced from Warlick et al. 2022): survival probabilities ϕ, state transition pupping probabilities ψ, detection probabilities p, and multi-event assignment probability δ for each age a for male and female wDPS Steller sea lions. (b) Directed acyclic graph: the integrated population model framework, including the subcomponent (i) multi-event model estimating demographic and detection probabilities for each age a and the number of breeding females N_B using resight data and the (ii) count model estimating the number of pups N_{pup} based on the pup index used here as input data (estimated by agTrend using raw count survey data) along with the population growth equations that unite them (upper right)

ers, $\psi_{N\text{-}B}$, describes the probability that a female that was a non-breeder in the previous year has a pup).

Spatio-temporally varying survival and pupping probabilities for each state were modeled as functions of fixed effects of natal subregion, environmental covariates, and smoothed random effects of year:

$$\text{logit}(\gamma_{a,s,r,t}) = \mu^{\gamma}_{a,s} + \mathbf{x}'\beta^{\gamma}_{a,r} + \varepsilon^{\gamma}_{a,r,t} \quad (2)$$

where $\gamma_{a,s,r,t}$ is a general demographic parameter for age a, sex s, region r, and year t; $\mu^{\gamma}_{a,s}$ is an age- and sex-specific intercept; $\mathbf{x}$ is a vector of covariates (including natal region and environmental variables) with associated coefficients $\beta^{\gamma}_{a,r}$; and $\varepsilon^{\gamma}_{a,r,t}$ is a smoothed annual random effect. We used informed priors to estimate age- and sex-specific demographic rates, where each $\mu^{\gamma}_{a,s}$ was assumed to be drawn from a Gaussian distribution with a mean and standard deviation based on similar age- and sex-specific survival and natality estimates from sea lions marked and resighted in southeast Alaska and Russia during the early 2000s (Hastings et al. 2018, A. Altukhov unpubl. data) (see our Text S1 and Table S1 in the Supplement at www.int-res.com/articles/suppl/n052p343_supp.pdf). These informed priors were used due to the high degree of uncertainty in demographic estimates for subregions west of Samalga Pass (largely due to the smaller number of cohorts informing age-specific survival and pupping in those subregions). Separate fixed effects of natal region were estimated for survival of pups, yearlings, age-2 individuals, and breeding females, and for pupping probabilities of age-3, age-4, and age-5 individuals, established breeders, and previous non-breeders. To improve estimability and reduce the number of model parameters, a pooled effect of natal region was estimated for the survival of male and female juvenile age groups (age-3, age-4, and age-5 individuals) for subregions in the eastern versus western portions of the wDPS range. The range-wide effect of environmental covariates (SST, NPGO) were estimated for the survival of male and female pups, yearlings, age-2 individuals, breeding females, and pupping probabilities for first-time and repeat breeders based on the assumption that those demographic rates would be the strongest drivers of population dynamics and most susceptible to environmental perturbation.

We applied penalized complexity (PC) priors (Simpson et al. 2017, van Erp et al. 2019) for defining prior distributions on fixed effects of natal region and environmental variables and on random year effects. This approach shrinks the coefficients toward zero in the absence of strong support for an effect and can improve parameter estimability and regulate model complexity. The PC priors for the fixed effects of natal region and environmental covariates were constructed by defining the conditional prior distribution $\beta^{\gamma}_{a,r} \sim N(0,\sigma_{\gamma_a})$ with standard deviations σ_{γ_a}, which were subsequently distributed according to an exponential distribution with a fixed shrinkage rate

$\sigma_{\gamma_a} \sim \text{Exp}(\lambda = 1)$ to apply moderately strong shrinkage. Random year effects were shared between sexes and estimated only for subregions in the eastern portion of the wDPS range (due to insufficient sample sizes in the central and western AI) using an intrinsic Gaussian conditional autoregressive (CAR) model prior distribution that enforced autocorrelation between years,

$$\boldsymbol{\epsilon}^{\gamma}_{a,r} \sim \text{MVN}(0, \sigma\mathbf{Q}) \quad (3)$$

where $\mathbf{Q}$ is the precision matrix of an intrinsic autoregression of order 2 (IAR(2); Speckman & Sun 2003) scaled by σ, and $\boldsymbol{\epsilon}^{\gamma}_{a,r}$ is a vector of temporal random effects, $\epsilon^{\gamma}_{a,r,t}$. The IAR(2) model imposes a smoothness constraint that reduces model complexity relative to independent random effects. For survival of pups, yearlings, age-2 individuals, and breeding females, separate random effects were estimated for each of the 4 subregions in the eastern portion of the wDPS range (western GoA-eastern AI). For survival of age-3, age-4, and age-5 males and females and pupping probabilities for age-4 individuals and established breeders, random year effects were shared across all 4 of the easternmost subregions. Temporal variability was not estimated for several demographic rates due to poor estimability, namely, nonbreeding female adult survival and first-time pupping probability for age-3 individuals, age-5 individuals, and previous non-breeders. As no individuals were marked in the western GoA during the study period, demographic rate estimates for that subregion were largely informed by modeled count data. This fixed and random effects model structure was chosen (among many other possible parameterizations) to balance the potential insights gained from enhanced spatio-temporal demographic information and the trade-off of greater uncertainty in the estimates. Demographic rates estimated here may differ from those reported in Warlick et al. (2022), who used the same mark-recapture data due to estimating regional effects and integrating modeled count data with little observation error.

The events in the multi-event model are defined by the possible observations of individuals. For all states except for breeding females, events are detected and not detected. For breeding females, events are as follows: seen without a pup, seen with a pup, or not detected. These events are modeled as

$$y_{i,t} \mid z_{i,t} \sim \text{categorical}(\Theta_{z_{i,t},i,t}) \quad (4)$$

where observations $y_{I,t}$ conditional on the true state $z_{I,t}$ are categorically distributed with observation array Θ, which is composed of an individual's detection probability at time t, $p_{I,t}$, and the probability of correctly ascertaining the presence of a pup for female breeders, $\delta_{I,t}$. Temporal variation was modeled as

$$\text{logit}(p_{a,s,t}) = \mu^{p}_{a,s} + \epsilon^{p}_{t} \quad (5)$$

where the mean intercept $\mu^{p}_{a,s}$ for each sex s and age a was estimated using a logit-transformed uniform (0,1) prior distribution. Interannual variability in detection probability was estimated with random year effects assumed to be drawn from a Gaussian distribution as $\epsilon^{p}_{t} \sim \text{N}(0,\sigma_p)$, with standard deviations σ_p distributed exponentially with a fixed shrinkage rate as described above. As in Warlick et al. (2022), we used the number of sightings per individual per year (with pups or without) as a categorical covariate for the multi-event classification probability parameter, $\delta_{i,t}$.

2.3.2. State-space model to estimate pup abundance

A state-space model was used to estimate pup abundance in year t in subregion r using the modeled posterior median and standard deviation of the modeled agTrend pup abundance index for all rookeries and haulout sites across the wDPS range (surveyed and unsurveyed):

$$N_{\text{pup}_{r,t}} \sim \text{normal}(N^{\text{F}}_{\text{pup}_{r,t}} + N^{\text{M}}_{\text{pup}_{r,t}}, \sigma^{\text{pup}}_{r,t}) \quad (6)$$

where annual pup abundance $\text{N}_{\text{pup}_{r,t}}$ in region r is normally distributed with a mean of annual pup abundance estimated in the stochastic population growth equations (Eq. 8) and variance $\sigma^{\text{pup}}_{r,t}$ equal to the known variance of the modeled agTrend abundance index (Sweeney et al. 2022). Although the sampling distribution of the estimated pup abundance indices possesses some temporal correlation, this is driven by the nonparametric trend model used in agTrend. To avoid undue influence of this trend model in the current population model analysis, we assumed no correlation between the annual estimates to make use of only marginal uncertainty in each year's pup abundance index.

2.3.3. IPM

The multi-event model was combined with the pup abundance model in an IPM framework using stochastic growth equations (Fig. 2b). The population process model was initialized 1 yr prior to the start of the mark-resight data (2000) using a discrete uniform distribution with minimum and maximum values set

at 75% and 125% of the expected counts based on the expected stable age distribution proportions. For example, for the number of breeding females in year 1 in region r, $N_{\mathrm{B}_{r,1}}$,

$$N_{\mathrm{B}_{r,1}} \sim \mathrm{uniform}(N_{\mathrm{min}_{r,1}} \cdot SA_{\mathrm{B}} \cdot 0.75,\ N_{\mathrm{min}_{r,1}} \cdot SA_{\mathrm{B}} \cdot 1.25) \quad (7)$$

where $N_{\mathrm{min}_{r,1}}$ is the sum of modeled pup and non-pup counts in each region in the initial year and SA_B is the proportion of breeders expected based on the stable age distribution calculated from the dominant eigenvalues of a Leslie matrix containing the range-wide demographic rates estimated in Warlick et al. (2022).

In each year $t + 1$, the number of pups for each sex was modeled as arising from a binomial distribution based on the number of breeding females and the assumption of an equal pup sex ratio. For all other ages and classes in each year $t + 1$, the number of individuals at a given age were modeled as arising from a Poisson distribution based on the number of individuals and survival and pupping probabilities in the previous year t:

$$\begin{bmatrix}
N^{\mathrm{F}}_{\mathrm{pup}_{r,t+1}} \sim \mathrm{Bin}(0.5, N^{\mathrm{F}}_{\mathrm{B}_{r,t+1}}) \\
N^{\mathrm{F}}_{1_{r,t+1}} \sim \mathrm{Pois}(N^{\mathrm{F}}_{\mathrm{pup}_{r,t}} \phi^{\mathrm{F}}_{\mathrm{pup}_{r,t}} \cdot m) \\
N^{\mathrm{F}}_{2_{r,t+1}} \sim \mathrm{Pois}(N^{\mathrm{F}}_{1_{r,t}} \phi^{\mathrm{F}}_{1_{r,t}}) \\
N^{\mathrm{F}}_{3_{r,t+1}} \sim \mathrm{Pois}(N^{\mathrm{F}}_{2_{r,t}} \phi^{\mathrm{F}}_{2_{r,t}}) \\
N^{\mathrm{F}}_{4_{r,t+1}} \sim \mathrm{Pois}(N^{\mathrm{F}}_{3_{r,t}} \phi^{\mathrm{F}}_{3_t} [1 - \psi_{3\text{–B}}]) \\
N^{\mathrm{F}}_{5_{r,t+1}} \sim \mathrm{Pois}(N^{\mathrm{F}}_{4_{r,t}} \phi^{\mathrm{F}}_{4_t} [1 - \psi_{4\text{–B}}]) \\
N^{\mathrm{F}}_{\mathrm{B}_{r,t+1}} \sim \mathrm{Pois}(N^{\mathrm{F}}_{3_{r,t}} \phi_{3_t} \psi_{3\text{–B}} + N^{\mathrm{F}}_{4_{r,t}} \phi_{4_t} \psi_{4\text{–B}} + N^{\mathrm{F}}_{5_{r,t}} \phi_{5_t} \psi_{5\text{–B}} \\
\qquad + N^{\mathrm{F}}_{\mathrm{B}_{r,t}} \phi_{B_t} \psi_{\mathrm{B–B}} + N^{\mathrm{F}}_{\mathrm{NB}_{r,t}} \phi_{\mathrm{NB}_t} \psi_{\mathrm{N–B}}) \\
N^{\mathrm{F}}_{\mathrm{B}_{r,t+1}} \sim \mathrm{Pois}(N^{\mathrm{F}}_{\mathrm{B}_{r,t}} \phi_{\mathrm{B}_t} [1 - \psi_{\mathrm{B–B}}] + N^{\mathrm{F}}_{\mathrm{NB}_{r,t}} \phi_{\mathrm{NB}_t} [1 - \psi_{\mathrm{N–B}}] \\
\qquad + N^{\mathrm{F}}_{5_{r,t}} \phi_{5_t} [1 - \psi_{5\text{–B}}]) \\
N^{\mathrm{M}}_{\mathrm{pup}_{r,t+1}} \sim \mathrm{Bin}(0.5, N^{\mathrm{F}}_{\mathrm{B}_{r,t+1}}) \\
N^{\mathrm{M}}_{1_{r,t+1}} \sim \mathrm{Pois}(N^{\mathrm{M}}_{\mathrm{pup}_{r,t}} \phi^{\mathrm{M}}_{\mathrm{pup}_{r,t}} \cdot m) \\
N^{\mathrm{M}}_{2_{r,t+1}} \sim \mathrm{Pois}(N^{\mathrm{M}}_{1_{r,t}} \phi^{\mathrm{M}}_{1_{r,t}}) \\
N^{\mathrm{M}}_{3_{r,t+1}} \sim \mathrm{Pois}(N^{\mathrm{M}}_{2_{r,t}} \phi^{\mathrm{M}}_{2_{r,t}}) \\
N^{\mathrm{M}}_{4_{r,t+1}} \sim \mathrm{Pois}(N^{\mathrm{M}}_{3_{r,t}} \phi^{\mathrm{M}}_{3_t}) \\
N^{\mathrm{M}}_{5_{r,t+1}} \sim \mathrm{Pois}(N^{\mathrm{M}}_{4_{r,t}} \phi^{\mathrm{M}}_{4_t}) \\
N^{\mathrm{M}}_{6_{r,t+1}} \sim \mathrm{Pois}(N^{\mathrm{M}}_{5_{r,t}} \phi^{\mathrm{M}}_{5_t}) \\
N^{\mathrm{M}}_{\mathrm{A}_{r,t+1}} \sim \mathrm{Pois}(N^{\mathrm{M}}_{5_{r,t}} \phi^{\mathrm{M}}_{5_t} + N^{\mathrm{M}}_{\mathrm{A}_{r,t}} \phi^{\mathrm{M}}_{\mathrm{A}_t})
\end{bmatrix} \quad (8)$$

Poisson distributions were used here instead of binomial distributions because a Poisson-distributed age structure offered more stability in the population model, improved convergence, approximated binomial outcomes given the large abundances, and theoretically allowed for a small degree of movement of individuals between subregions given that individuals are occasionally resighted outside their natal subregions (i.e. it was possible, but not probable, that $N_{a+1_{r,t+1}} > N_{a_{r,t}}$). Total abundance in each year and subregion was then calculated as the sum of individuals in all age classes a and states, $N_{\mathrm{Tot}_{r,t}} = \sum(N_{a_{r,t}})$. Due to lack of data to estimate it, neonate mortality m (i.e. the mortality that occurs between birth and the aerial survey versus marking) was assumed to be 5% (Merrick 1987), though this value likely varies considerably from year to year (Maniscalco et al. 2008).

2.4. Growth rates, sensitivity, and viability analyses

For each of the 6 management subregions, we calculated the correlation coefficient (r) between posterior mean annual population growth rates (λ_t) and annual age-specific female survival and pupping rates to examine the sensitivity of population growth rates to each vital rate.

To examine the viability of populations in each of the 6 management subregions, we projected the population forward in time for $T = 100$ yr using the posterior distributions of the vital rate parameters estimated for the timeframe informed by mark-resight data (2000–2018). For each year in the 100 yr projection period, we randomly selected posterior samples of the random deviates from one of the 18 study years informed by data (with replacement) and added this to posterior samples of the corresponding intercept term and randomly generated SST and NPGO values for a given year t. The resulting value was inverse logit-transformed to derive demographic rates for use in population growth equations (as above, Eq. 8, without density dependence mechanisms) to calculate stage-specific abundance at each $t + 1$. Due to the complex and variable nature of a top predator's response to environmental conditions, the comparison of projection scenarios is intended not as a predictive tool but instead to provide a general sense of how meaningful system change (e.g. under climate change) might impact population growth rates via the underlying demography. Posterior distributions of the population projections were summarized in terms of the average population growth rate, $\lambda_t = \frac{N_{\mathrm{Tot}_{t+1}}}{N_{\mathrm{Tot}_t}}$; the probability of local extirpation, $\Pr(N_{\mathrm{Tot}} < 1)$; the probability of having no remaining breeding females, $\Pr(N_{\mathrm{B}} < 1)$; and the probability of experiencing positive population growth. To compare the estimation of abundance using the IPM versus alternative estimation or relative index approaches, we compared the population growth rates derived using abundance

estimates from the IPM and those calculated using the N_{min} (sum of agTrend-modeled pup and non-pup counts) and 'pup multiplier' (agTrend-modeled pup counts multiplied by a fixed ratio: $w = \frac{N_{Tot}}{N_{pup}}$) approaches. The N_{min} approach has been used to calculate potential biological removal levels for authorizing takes under the Marine Mammal Protection Act (MMPA). The pup multiplier approach was previously employed to estimate abundance and trends, with a multiplier ratio assumed to be a fixed value of $w = 4.5$, developed based on a stable age distribution assumption (Calkins & Pitcher 1982).

2.5. Model assumptions and fitting

For the multi-event model, the typical set of mark-recapture model assumptions applies, including that branding had a negligible effect on survival (Hastings et al. 2009) and detection probabilities, that there were no identification errors, that mortality during the sampling season was negligible, that individuals were independent, that there was no unmodeled heterogeneity in survival and detection probabilities, and that marked individuals are representative of the population of interest. Lack-of-fit issues were not apparent in the analysis of these data in Warlick et al. (2022). For the abundance model, we assumed that there were no errors in classifying pups and that the pup count is nearly a complete census, as the surveys occur when pups are still onshore.

The IPM was fit using NIMBLE (NIMBLE Development Team 2019) within the R programming environment (R Core Team 2022) using 45 000 iterations, 20 000 burn-in, and an adaptation rate of 10. Convergence was evaluated using visual inspection of chains and the Brooks-Gelman-Rubin statistic $\hat{R} < 1.1$ (Gelman & Rubin 1992, Brooks & Roberts 1998) calculated using the *gelman.diag* function in the coda R package (Plummer et al. 2006). Population projections were carried out in R using the Markov chain Monte Carlo (MCMC) samples.

3. RESULTS

3.1. Vital rates

Age-specific vital rates varied notably by region. Female pup survival (ϕ_P) was lower in the central AI (0.31, 95% credible interval [CI]: 0.24–0.41) and higher in the western AI (0.71, 0.62–0.81), with a wDPS range-wide average of 0.54 (0.38–0.75; Fig. 3). Pup survival rates in each of the 4 subregions where we were able to estimate temporally varying survival (GoA and eastern AI) were lower toward the end of the study period (Fig. 4). Female yearling survival (ϕ_1) was notably lower in the central AI (0.49, 0.28–0.71) and western AI (0.59, 0.46–0.73), with a range-wide average of 0.72 (0.54–0.87). Male pup and yearling survival was slightly lower than that of females but followed similar regional and temporal patterns (Text S2, Figs. S1 & S2). Survival of older juveniles (ϕ_3, ϕ_4, ϕ_5) did not vary notably across the subregions but exhibited a slightly negative trend over the study period. Adult female breeding survival (ϕ_B) was relatively similar across subregions, with a slightly lower average rate in the eastern portion of the wDPS range, where rates declined between 2000 and 2008 (Fig. 4). Age-specific first-time pupping probability was highest for age-5 individuals (ψ_{4-B}) and similar across regions. The probability of pupping for age-4 individuals (ψ_{3-B}) was lower in the eastern portion of the wDPS range and higher in the western portion relative to the range-wide average (Fig. 3). The probability of pupping for repeat breeders (ψ_{B-B}) increased from eastern to western subregions, with the exception of the western AI, where the rate was lowest. Pupping probabilities for repeat breeders were lower in the last several years of the study period, while the probability of first-time pupping for age-5 individuals was lower in the mid-2000s (Fig. 4). Due to smaller sample branding cohort sizes over shorter time horizons in the western and central AI, some stage- and region-specific pupping probabilities were not estimated well in certain cases.

3.2. Population growth rates, abundance, and age structure

Over the study period, the range-wide abundance of the wDPS increased from 33 568 (95% CI: 31 430–35 723) in 2000 to 48 278 (43 267–53 900) in 2021, representing an average growth rate of 1.74% (0.14 to 3.45%) yr^{-1} (Figs. 5 & 6). However, abundance trends in each of the subregions varied, with an increasing abundance trend in the subregions in the eastern portion of the wDPS and a decreasing trend in the central and western AI subregions (Fig. 5). The mean annual population growth rate was highest in the eastern AI (3.7%, 95% CI: 0.53 to 7.00%), followed by the western GoA (3.40%, 1.02 to 6.67%), the central GoA (3.04%, –0.46 to 6.60%), and the eastern GoA (1.76%, –2.60 to 6.47%). The mean annual pop-

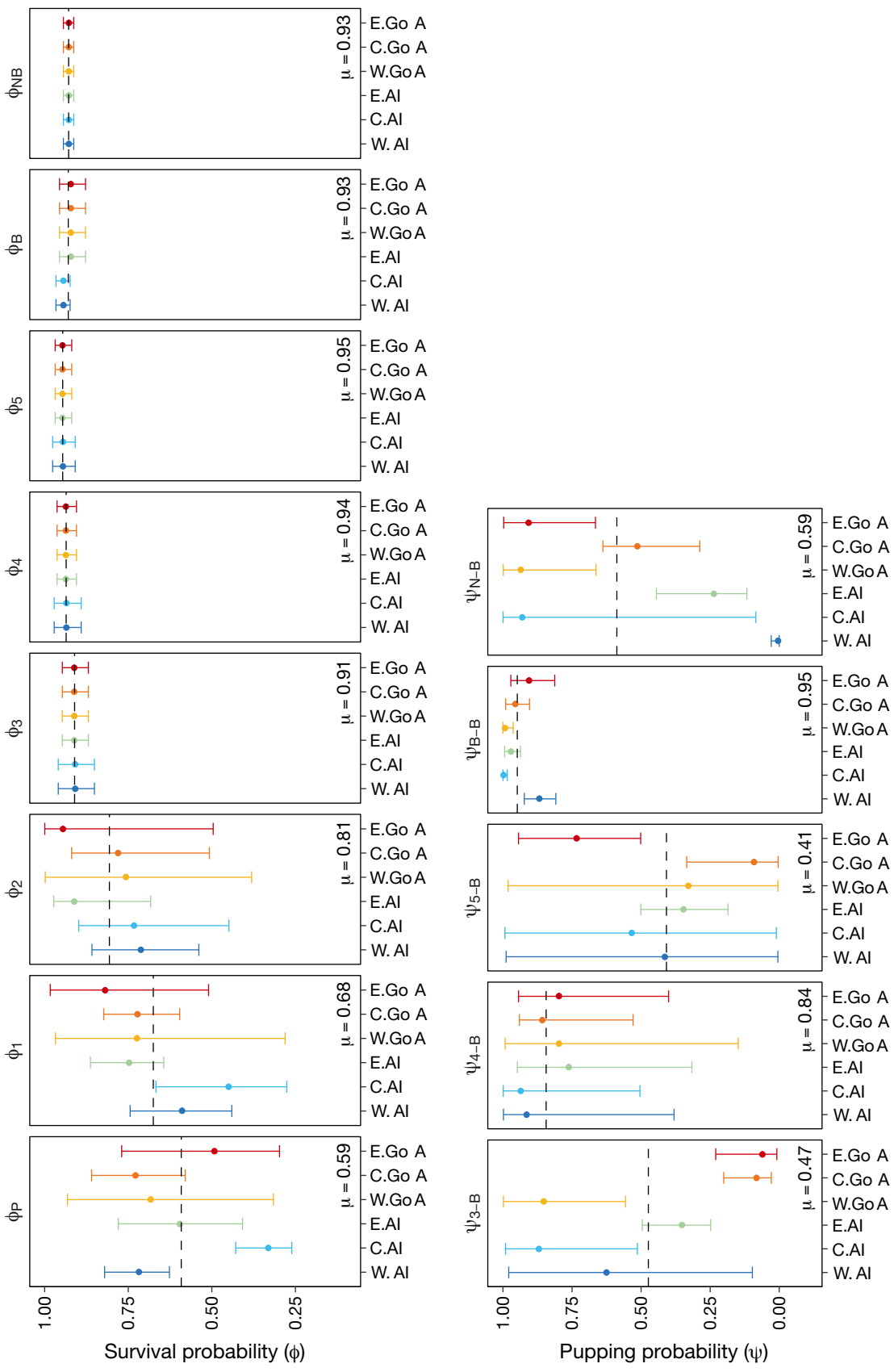

Fig. 3. Posterior mean and 95% credible intervals for age-specific survival (ϕ) and first-time ($\psi_{3\text{-}B:5\text{-}B}$) and repeat ($\psi_{B\text{-}B,N\text{-}B}$) pupping probabilities for female Steller sea lions across the 6 western distinct population segment subregions (W.AI: western Aleutians; C.AI: central Aleutians; E.AI: eastern Aleutians; W.GoA: western Gulf of Alaska; C.GoA: central Gulf of Alaska; E.GoA: eastern Gulf of Alaska). Dashed line: range-wide average. Male survival rates are provided in Text S2 and Figs. S1 & S2 in the Supplement

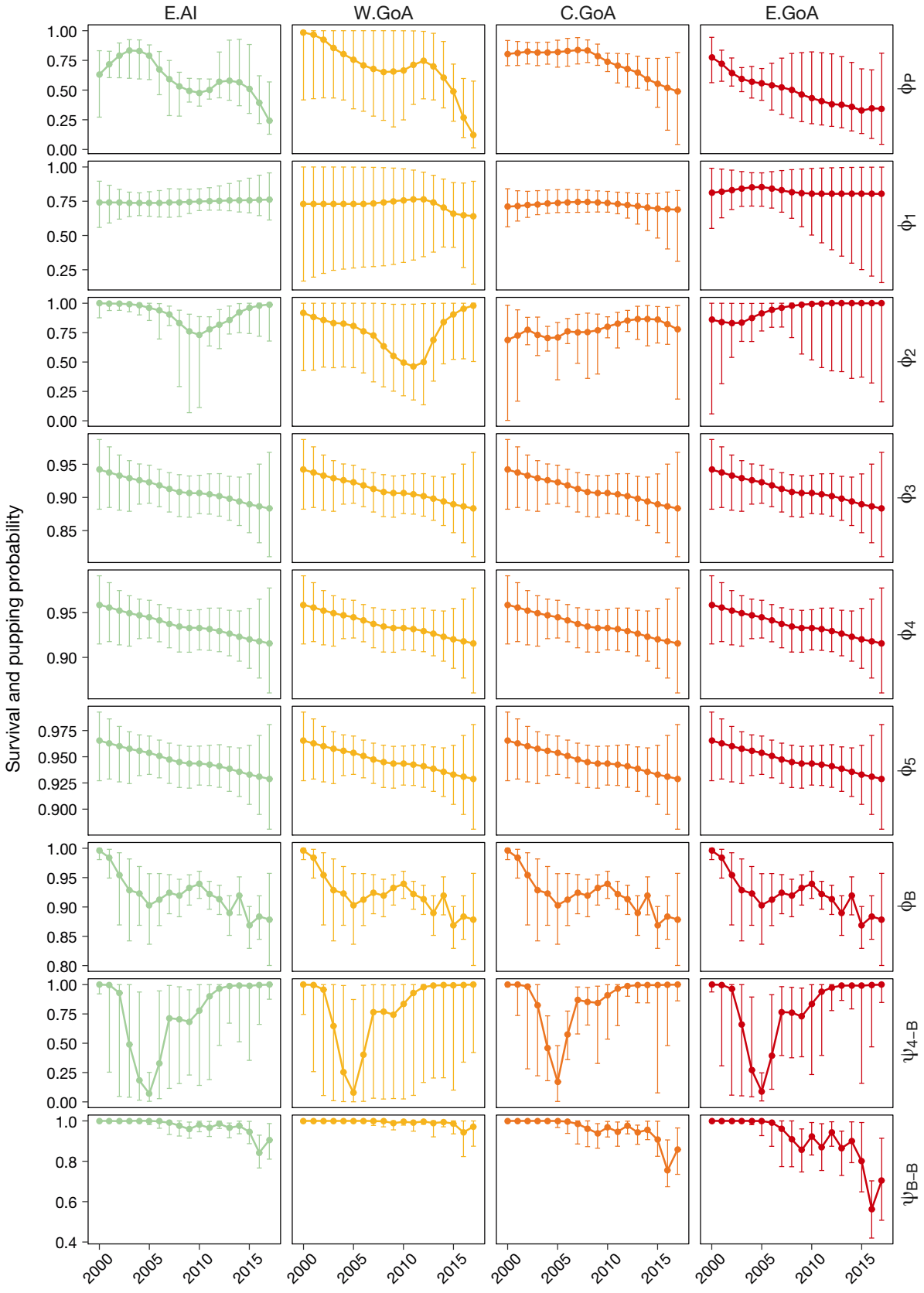

Fig. 4. Posterior mean and 95% credible intervals for time-varying Steller sea lion female age-specific survival ($\phi_{P,1:5,B}$) and first-time ($\psi_{4\text{-}B}$) and repeat ($\psi_{B\text{-}B}$) pupping probabilities across 4 of the western distinct population segment subregions (see Fig. 3 for abbreviations)

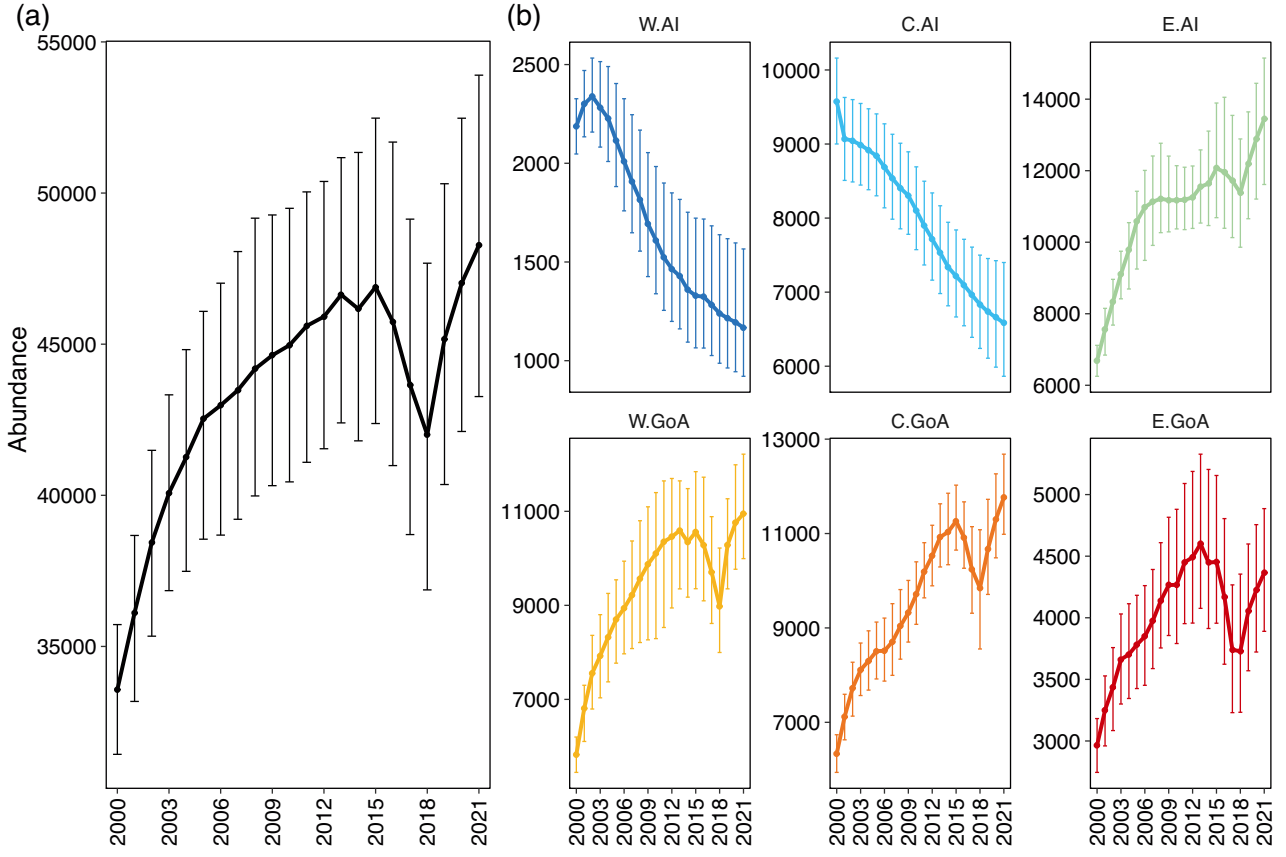

Fig. 5. Posterior mean and 95% credible intervals for total abundance of Steller sea lions: (a) range-wide and (b) in the 6 western distinct population segment subregions (see Fig. 3 for abbreviations)

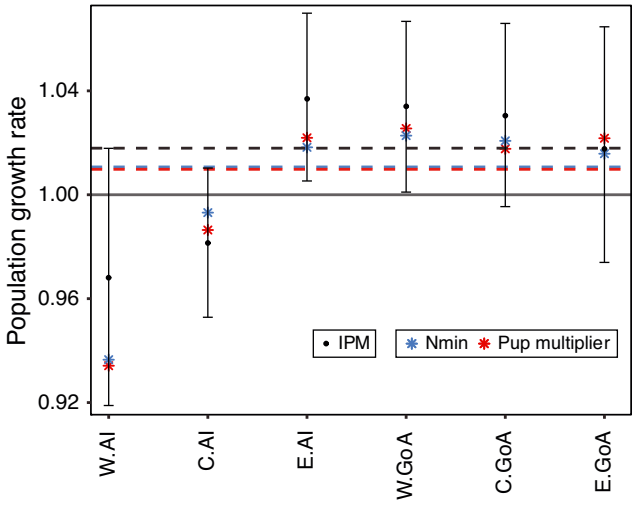

Fig. 6. Posterior mean and 95% credible intervals of Steller sea lion population growth rates in the 6 western distinct population segment subregions (see Fig. 3 for abbreviations) and range-wide (dashed lines) based on abundance estimates from the integrated population model (IPM), and from agTrend-modeled N_{min} and agTrend-modeled 'pup multiplier' approaches (as described in Section 2.4)

ulation growth rate was lowest, and negative, in the central AI (–1.86%, –4.72 to 1.03%) and western AI (–3.19%, –8.11 to 1.79%) (Fig. 6).

The average age class distribution over the study period across the 6 subregions was approximately 20% pups, 20% breeding females, 12% yearlings, 19.1% juveniles, 5.6% non-breeding females, and 15.4% adult males. However, there were a few notable exceptions, including lower proportions of pups and female breeders in the western AI relative to the range-wide estimates (Fig. S2). In contrast, in the central AI, there were higher proportions of pups and breeding females and lower proportions of yearlings and juveniles. In the wDPS as a whole, the $\frac{N_{Tot}}{N_{pup}}$ ratio was approximately 4.4 (95% CI: 3.2–5.4) but varied over time, degree of uncertainty, and across the 6 subregions (Fig. 7). Specifically, this ratio was much lower (indicating higher number of pups relative to non-pups) than the range-wide average in central AI, and much higher (indicating lower number of pups) than the range-wide average in the western AI.

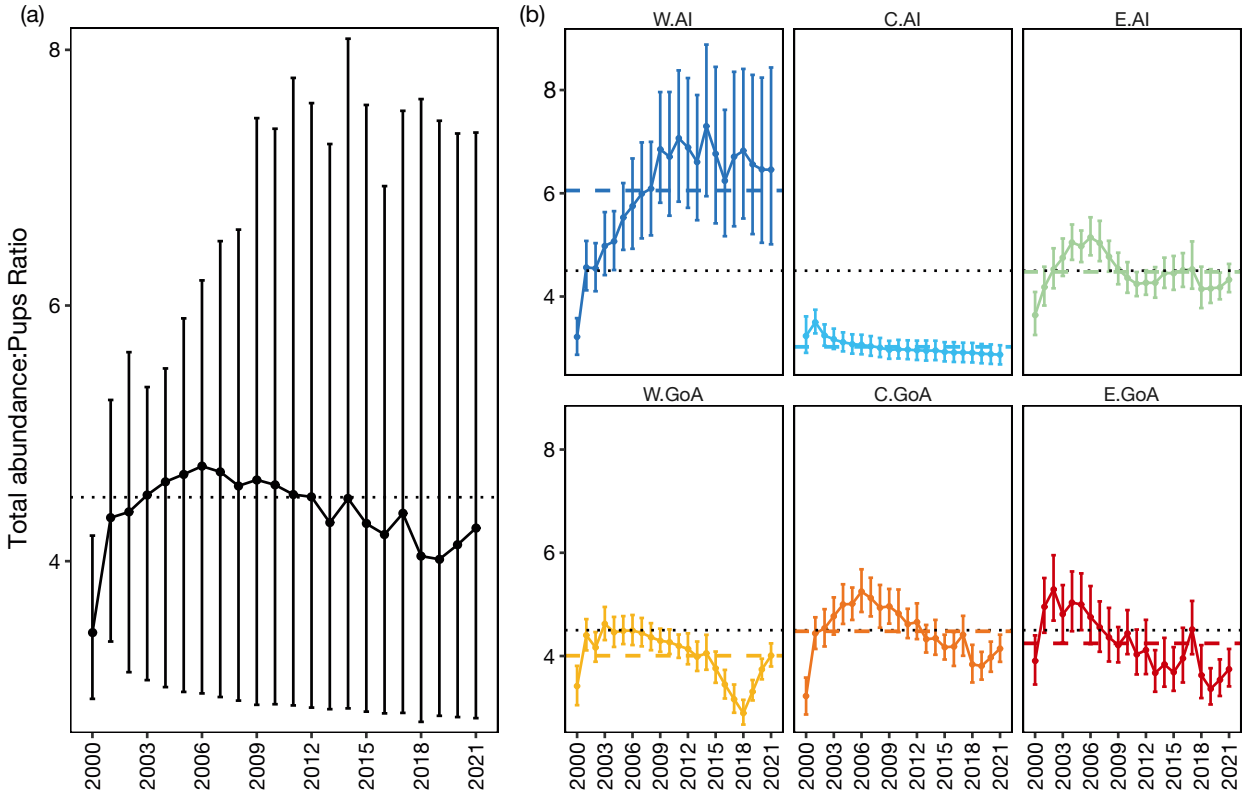

Fig. 7. Posterior mean and 95% credible intervals of the ratio of total abundance to pup abundance: (a) range-wide and (b) in each of the 6 western distinct population segment subregions (see Fig. 3 for abbreviations), with the traditional 4.5 'pup multiplier' (black dotted line) and the regional averages (colored dashed lines)

3.3. Sensitivity, viability, and covariate effects

Demographic rates were generally positively correlated with population growth rates (Text S2, Figs. S4 & S5). The highest correlation coefficients, with credible intervals that did not overlap zero were estimated between population growth rates and both repeat breeding and female breeder survival probabilities (Fig. S4), though the correlations varied by subregion (Fig. S5).

Based on demographic rates estimated for the timeframe informed by data, projected abundance increased in subregions east of Samalga Pass and declined in the western subregions over the 100 yr time horizon. In the absence of additional movement between subregions, the probability of local extirpation in 100 yr was close to zero for the subregions, with increasing population trends in the eastern portion of the wDPS range and in the central AI, but was approximately 2% (95% CI: 1.7–2.5%) in the western AI. Similarly, the probability of having no remaining female breeders was effectively zero in all subregions except the western AI (11.5%, 10.7–12.6%). The probability of a negative abundance trend was close to zero for all subregions in the eastern portion of the wDPS range but was approximately 99.2% and 100% for the central and western AI subregions, respectively.

The estimated effects of summer SST (β_{SST}) and NPGO (β_{NPGO}) conditions on pupping probability (ψ_B) and the survival of pups (ϕ_P) and yearlings (ϕ_1) were positive (Text S2, Fig. S3). Our prediction scenarios indicated that adjusting the mean of environmental covariates drove the greatest percent changes in population growth rates compared with adjusting the variability (Table 1). However, the magnitude of the change in population growth rates varied based on the underlying demography in each of the 6 subregions, with particularly notable effects in the western AI, where rates of decline were lower in scenarios with less variability and warmer SST and warm-phase NPGO conditions, and higher with wider credible intervals in scenarios with greater variability and lower mean SST and cool-phase NPGO relative to baseline conditions (Fig. 8).

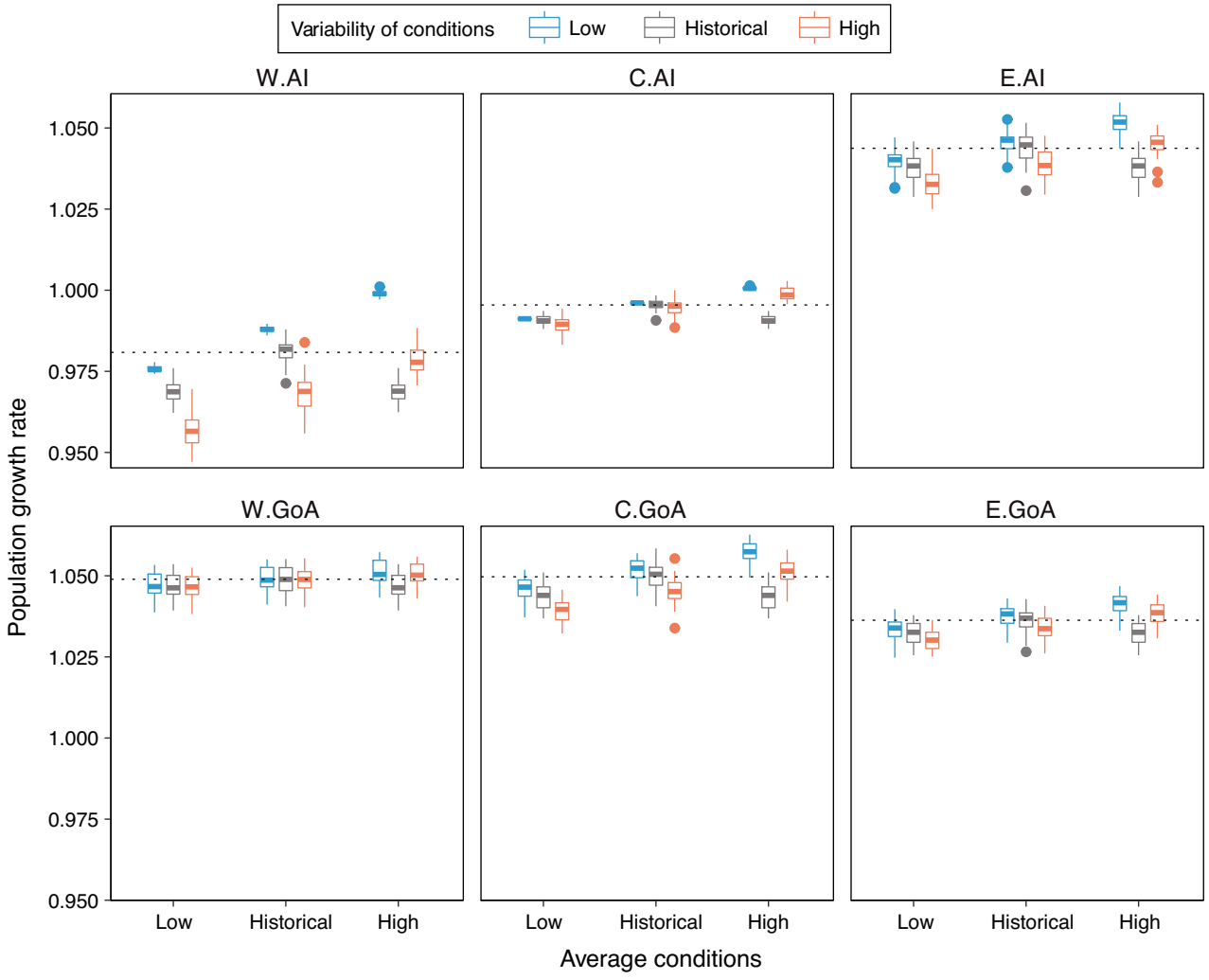

Fig. 8. Population growth rates for Steller sea lions in the western distinct population segment, by subregion (see Fig. 3 for abbreviations) during the population projection period (2022–2122) across projection scenarios with varying mean and standard deviation of generated sea surface temperature and North Pacific Gyre Oscillation predictor variables compared with the baseline scenario that adopts the mean and variability of historical conditions (dotted line). Solid line: median; upper and lower box hinges: first and third quartiles; whisker extents: minimum and maximum values; points: outliers. See Sections 2.2 & 2.4, and Table 1 for details on the projection scenarios

4. DISCUSSION

We combined mark-resight data and annual pup abundance estimates from aerial surveys to examine the demographic factors underlying divergent abundance trends across the 6 management subregions in the range of the wDPS of Steller sea lions. We undertook this analysis to (1) identify regional differences in vital rates that may be driving divergent abundance trends, (2) improve upon the existing approach of estimating abundance, and (3) present a framework for examining the sensitivity of population dynamics and viability to regional demography and environmental variability. Our results indicated that sea lion population dynamics vary due to regional demographic differences, temporal variance, and environmental factors. This information can inform future research and monitoring priorities and allow managers to evaluate progress toward recovery goals for this population.

Understanding regional differences in survival and natality over time and across the wDPS range is fundamental to gaining insights about the drivers of observed abundance trends. Empirical evidence and ecological theory suggest that population dynamics are generally most sensitive to changes in adult survival (Heppell et al. 2000, Runge et al. 2004, Gormley et al. 2012), but also to fecundity and offspring survival, as these rates tend to be more variable (Manlik et al. 2016, Lacy et al. 2017). Our results indicated

that populations to the west of Samalga Pass may be declining via 2 different demographic mechanisms. In the central AI, pup and yearling survival was relatively low during the study period and apparently not offset by higher reproductive rates. In contrast, in the western AI, the decline may be driven by lower survival of age-1 and age-2 individuals, as the lower reproductive rates combined with relatively higher pup survival suggest high maternal investment. However, the ways in which demographic drivers may have changed over time are less clear. Though our IPM facilitated the estimation of temporal variance in vital rates in subregions east of Samalga Pass (showing lower repeat pupping and survival rates for pups and breeding females during the latter part of the study period), cohort sample sizes did not support the estimation of independent annual pupping rates west of Samalga Pass, making it difficult to understand the role of natality in driving population dynamics in those subregions where uncertainty is particularly high. Taken together, this study provides additional insights into how the demographic factors driving changes in abundance are likely variable across subregions and change over time, as has been suggested by previous studies (Holmes & York 2003, Holmes et al. 2007).

An improved understanding of a population's sensitivity to environmental perturbation is fundamental to the assessment of threats under the US ESA. Despite the complexities of quantifying the effects of ocean conditions on long-lived top predators, our illustrative example highlights the importance of understanding the effects of environmental variability on population viability. Under scenarios where environmental conditions (i.e. NPGO and SST) were projected to remain similar to historical conditions, the probability of local extirpation for the western and central AI subregions was still relatively low (<2%), though the 100 yr time horizon is relatively short for a long-lived mammal and there was a high probability of a continued declining trend. These findings were broadly consistent with previous viability analyses that found a low overall probability of extinction, with results varying widely depending on model assumptions and lower rates of persistence for certain rookeries (York et al. 1996, Gerber & VanBlaricom 2001, Winship & Trites 2006). In terms of the effects of environmental variability, our results revealed that the potential effects of changing oceanographic conditions were largest in the western AI subregion, where the population is smallest and key demographic rates, namely survival of pups and yearlings and pupping probabilities, were depressed relative to the range-wide average. In other words, the regional response to environmental perturbation is dependent on the magnitude of the covariate effect as well as baseline demographic rates, age structure, and population size. This IPM-PVA model structure represents the best use of available information about the population, which can reduce uncertainty in model estimates and therefore improve our understanding of future population dynamics, as the reliability of PVA extinction probabilities can be questionable over longer time horizons (Fieberg & Ellner 2000). However, future studies could expand upon this analysis by estimating more nuanced region-specific covariate effects, including temporal lags in the effects of ocean conditions and a changing frequency of extreme conditions.

Vital rate and abundance estimates are common metrics for assessing a population's conservation status and evaluating the efficacy of conservation management policies designed to maintain the resilience of stable populations or recover depleted ones. However, obtaining precise and unbiased estimates of these parameters can be challenging for marine mammals due to the high cost of surveys, small sample sizes, and the longer time series needed for long-lived organisms (Taylor et al. 2007, Boyd & Punt 2021). For Steller sea lions, their ESA listing status is largely dependent on estimates of subregional population trends. While the 'pup multiplier' or a relative index of abundance (e.g. N_{min}) can serve as convenient metrics for population monitoring (particularly when and where abundance cannot be estimated), our IPM-based PVA model provides a more robust framework that accounts for uncertainty in female reproductive state and imperfect detection in mark-resight and aerial surveys. While the mean $\frac{N_{Tot}}{N_{pup}}$ ratio estimated in this study was approximately 4.4 (95% CI: 3.2–5.4), similar to the traditional 4.5 'pup multiplier', a closer examination of the subregional and temporal variability in that ratio revealed how using it as an abundance multiplier may lead to inaccurate abundance estimates and biased population growth rates for certain regions or time periods when population structure may render this ratio inaccurate. This was particularly evident for the central and western AI subregions, where growth rates derived using the pup multiplier or index approaches would be over- and under-estimated, respectively (Fig. 6). The growth rates derived using modeled pup and/or non-pup counts are important factors in ESA listing decisions and MMPA take authorizations for the wDPS and could become increasingly biased (relative to estimates from a fully

integrated approach) for subregions where abundance continues to decline.

Our model framework corroborates existing abundance trends (Sweeney et al. 2022) that show continuing decline in the western subregions of the wDPS Steller sea lion range. The reasons for this continued decline remain largely unknown. Our results highlight subregional vital rates that may be depressed, which could reinforce the need to examine the efficacy of existing conservation measures and inspire discussion of whether any additional region-specific actions could be implemented to promote recovery. Identifying specific causal environmental mechanisms driving changes in vital rates was not the intention of this study and remains a challenge for conservation biologists monitoring the abundance of highly mobile, long-lived top predators, particularly those that exhibit divergent abundance trends across a large geographic range. The responses of ecosystem processes and demography to perturbations are often variable and difficult to predict (Zhao et al. 2019), and situations where wildlife populations are experiencing persistent unexplained declines or fluctuations in abundance may become more widespread in the future, given anticipated climate change (Pacifici et al. 2015, Poloczanska et al. 2016). A more refined understanding of demography often facilitated by integrated population modeling can improve the quality of information available for decision-making and evaluating progress toward recovery goals under the ESA. Our model and viability framework can also be used to examine the population-level effects of other stressors such as disease or contaminants when data become available in the future. Integrated population modeling facilitates reducing and accounting for all sources of uncertainty when examining the effects of natural or anthropogenic stressors on the population dynamics and viability of declining or depleted populations, which will become increasingly important given anticipated climate variability and change, where the threats and solutions are both global in scope.

Data availability. The data and code to reproduce these analyses are available on GitHub (doi:10.5281/zenodo.8432569).

Acknowledgements. We thank the staff of the NOAA Fisheries Alaska Fisheries Science Center Marine Mammal Lab and other institutions for the effort and time dedicated to mark-resight and aerial survey fieldwork, which was conducted under MMPA and ESA permit numbers 782-1532-00, 782-1532-01, 782-1532-02, 782-1532-03, 782-1768-00, 782-1768-01, 782-1889, 14326, 14326-01, 14326-02, 18528, and 22289, and animal care and use committee approvals A/NW 2010-4, A/NW 2013-2, and A/NW 2016-3. The findings and conclusions of the NOAA authors in the paper are their own and do not necessarily represent the views of the National Marine Fisheries Service or NOAA. Any use of trade, firm, or product names is for descriptive purposes only and does not imply endorsement by the US Government.

LITERATURE CITED

Abadi F, Gimenez O, Ullrich B, Arlettaz R, Schaub M (2010) Estimation of immigration rate using integrated population models. J Appl Ecol 47:393–400

Abadi F, Barbraud C, Gimenez O (2017) Integrated population modeling reveals the impact of climate on the survival of juvenile emperor penguins. Glob Change Biol 23:1353–1359

Arimitsu ML, Piatt JF, Hatch S, Suryan RM and others (2021) Heatwave-induced synchrony within forage fish portfolio disrupts energy flow to top pelagic predators. Glob Change Biol 27:1859–1878

Beissinger SR, Westphal MI (1998) On the use of demographic models of population viability in endangered species management. J Wildl Manag 62:821–841

Besbeas P, Freeman SN, Morgan B, Catchpole EA (2002) Integrating mark-recapture-recovery and census data to estimate animal abundance and demographic parameters. Biometrics 58:540–547

Bled F, Belant JL, Daele LJV, Svoboda N, Gustine D, Hilderbrand G, Barnes VG (2017) Using multiple data types and integrated population models to improve our knowledge of apex predator population dynamics. Ecol Evol 7:9531–9543

Boveng PL, Hoef JMV, Withrow DE, London JM (2018) A Bayesian analysis of abundance, trend, and population viability for harbor seals in Iliamna Lake, Alaska. Risk Anal 38:1988–2009

Boyd C, Punt AE (2021) Shifting trends: detecting changes in cetacean population dynamics in shifting habitat. PLOS ONE 16:e0251522

Brooks SP, Roberts GO (1998) Convergence assessment techniques for Markov chain Monte Carlo. Stat Comput 8:319–335

Brooks SP, King R, Morgan BJT (2004) A Bayesian approach to combining animal abundance and demographic data. Anim Biodivers Conserv 27:515–529

Calkins DG, Pitcher KW (1982) Population assessment, ecology and trophic relationships of Steller sea lions in the Gulf of Alaska. Environmental Assessment of the Alaskan Continental Shelf. Alaska Department of Fish and Game, Anchorage, AK. Final Reports 19:455–546

Champagnon J, Lebreton JD, Drummond H, Anderson DJ (2018) Pacific Decadal and El Niño oscillations shape survival of a seabird. Ecology 99:1063–1072

Cleasby IR, Bodey TW, Vigfusdottir F, McDonald JL and others (2017) Climatic conditions produce contrasting influences on demographic traits in a long-distance Arctic migrant. J Anim Ecol 86:285–295

Di Lorenzo E, Schneider N, Cobb KM, Chhak K and others (2008) North Pacific Gyre Oscillation links ocean climate and ecosystem change. Geophys Res Lett 35:L08607

Fieberg J, Ellner SP (2000) When is it meaningful to estimate an extinction probability? Ecology 81:2040–2047

Fritz LW, Stinchcomb C (2005) Aerial, ship, and land-based surveys of Steller sea lions (*Eumetopias jubatus*) in the western stock in Alaska, June and July 2003 and 2004. US Department of Commerce. NOAA Tech Memo NMFS-AFSC-153

Fritz L, Sweeney K, Towell R, Gelatt T (2016) Aerial and ship-based surveys of Steller sea lions (*Eumetopias jubatus*) conducted in Alaska in June-July 2013 through 2015, and an update on the status and trend of the western distinct population segment in Alaska. US Department of Commerce. NOAA Tech Memo NMFS-AFSC-321

Gaos A, Kurpita L, Bernard H, Sundquist L and others (2021) Hawksbill nesting in Hawai'i: 30-Year dataset reveals recent positive trend for a small, yet vital population. Front Mar Sci 8:770424

Gelman A, Rubin DB (1992) Inference from iterative simulation using multiple sequences. Stat Sci 7:457–472

Gerber LR, VanBlaricom GR (2001) Implications of three viability models for the conservation status of the western population of Steller sea lions (*Eumetopias jubatus*). Biol Conserv 102:261–269

Gormley AM, Slooten E, Dawson S, Barker RJ, Rayment W, du Fresne S, Bräger S (2012) First evidence that marine protected areas can work for marine mammals. J Appl Ecol 49:474–480

Hastings KK, Gelatt TS, King JC (2009) Postbranding survival of Steller sea lion pups at Lowrie Island in southeast Alaska. J Wildl Manag 73:1040–1051

Hastings KK, Jemison LA, Pendleton GW (2018) Survival of adult Steller sea lions in Alaska: senescence, annual variation and covariation with male reproductive success. R Soc Open Sci 5:170665

Heppell SS, Caswell H, Crowder LB (2000) Life histories and elasticity patterns: perturbation analysis for species with minimal demographic data. Ecology 81:654–665

Himes Boor GK, McGuire TL, Warlick AJ, Taylor RL, Converse SJ, McClung JR, Stephens AD (2022) Estimating reproductive and juvenile survival rates when offspring ages are uncertain: a novel multievent mark-resight model with beluga whale case study. Methods Ecol Evol 14:631–642

Holmes EE, York AE (2003) Using age structure to detect impacts on threatened populations: a case study with Steller sea lions. Conserv Biol 17:1794–1806

Holmes EE, Fritz LW, York AE, Sweeney K (2007) Age-structured modeling reveals long-term declines in the natality of Western Steller sea lions. Ecol Appl 17: 2214–2232

Jenouvrier S, Holland M, Iles D, Labrousse S and others (2019) The Paris Agreement objectives will likely halt future declines of emperor penguins. Glob Change Biol 26:1170–1184

Johnson DS, Fritz LW (2014) agTrend: a Bayesian approach for estimating trends of aggregated abundance. Methods Ecol Evol 5:1110–1115

Kendall WL, Langtimm CA, Beck CA, Runge MC (2004) Capture-recapture analysis for estimating manatee reproductive rates. Mar Mamm Sci 20:424–437

Kilduff DP, Lorenzo ED, Botsford LW, Teo SLH (2015) Changing central Pacific El Niños reduce stability of North American salmon survival rates. Proc Natl Acad Sci USA 112:10962–10966

Kuhn CE, Chumbley K, Johnson D, Fritz L (2017) A re-examination of the timing of pupping for Steller sea lions *Eumetopias jubatus* breeding on two islands in Alaska. Endang Species Res 32:213–222

Lacy RC, Williams R, Ashe E, Balcomb KC III and others (2017) Evaluating anthropogenic threats to endangered killer whales to inform effective recovery plans. Sci Rep 7:14119

Ladd C, Hunt GL, Mordy CW, Salo SA, Stabeno PJ (2005) Marine environment of the eastern and central Aleutian Islands. Fish Oceanogr 14:22–38

Litzow MA, Ciannelli L, Puerta P, Wettstein JJ, Rykaczewski RR, Opiekun M (2018) Non-stationary climate–salmon relationships in the Gulf of Alaska. Proc R Soc B 285: 20181855

Loughlin TR (1997) Using the phylogeographic method to identify Steller sea lion stocks. Mol Genet Mar Mamm 3: 159–171

Maniscalco JM (2018) NOAA/NMFS 5-year status review for Endangered Steller sea lions — comments. In: Cheever E, Riley T (2019) Steller sea lion thirty year review: bibliography. National Oceanic and Atmospheric Administration, Silver Spring, MD

Maniscalco JM, Calkins DG, Parker P, Atkinson S (2008) Causes and extent of natural mortality among Steller sea lion (*Eumetopias jubatus*) pups. Aquat Mamm 34: 277–287

Manlik O, McDonald JA, Mann J, Raudino HC and others (2016) The relative importance of reproduction and survival for the conservation of two dolphin populations. Ecol Evol 6:3496–3512

Martin M, McLaren A, Good S (2019) Product user manual for global ocean GMPE sea surface temperature multi product ensemble SST_GLO_SST_L4_NRT_OBSERVATIONS_010_005 16. Copernicus Marine Service, Toulouse

Merrick RL (1987) Behavioral and demographic characteristics of northern sea lion rookeries. MSc thesis, Oregon State University, Corvallis, OR

Merrick RL, Loughlin TR, Calkins DG (1996) Hot branding: a technique for long-term marking of pinnipeds. NOAA Tech Memo NMFSAFSC-68. NOAA, Seattle, WA

Mosnier A, Doniol-Valcroze T, Gosselin JF, Lesage V, Measures LN, Hammill MO (2015) Insights into processes of population decline using an integrated population model: the case of the St. Lawrence Estuary beluga (*Delphinapterus leucas*). Ecol Model 314:15–31

NIMBLE Development Team (2019) NIMBLE: MCMC, particle filtering, and programmable hierarchical modeling. R package version 1.0.1

NMFS (National Marine Fisheries Service) (1993) Designated critical habitat; Steller sea lion: Final Rule. 50 CFR Part 226. National Oceanic and Atmospheric Administration, Department of Commerce. 58 FR 45269

NMFS (2001) Endangered Species Act – Section 7 consultation biological opinion and incidental take statement: authorization of Gulf of Alaska groundfish fisheries based on the fishery management plan for the Bering Sea/Aleutian Islands groundfish as modified by amendments 61 and 70. NMFS Protected Resources Division, Silver Spring, MD

NMFS (2008) Recovery plan for the Steller sea lion (*Eumetopias jubatus*), revision. National Marine Fisheries Service. NMFS, Silver Spring, MD

NMFS (2020) Western distinct population segment Steller sea lion (*Eumetopias jubatus*) 5-year review: summary and evaluation. NMFS Protected Resources Division, Juneau, AK

NOAA NCEI (NOAA National Centers for Environmental Information) (2020) NOAA climate monitoring teleconnections: Arctic Oscillation. www.ncdc.noaa.gov/teleconnections/ao/ (accessed July 1, 2020)

NOAA PSL (NOAA Physical Sciences Laboratory) (2020) Gridded climate datasets. https://psl.noaa.gov/data/gridded/tables/ocean.html (accessed July 1, 2020)

O'Corry-Crowe G, Taylor BL, Gelatt T, Loughlin TR and others (2006) Demographic independence along ecosystem boundaries in Steller sea lions revealed by mtDNA analysis: implications for management of an endangered species. Can J Zool 84:1796–1809

Ohlberger J, Scheuerell MD, Schindler DE (2016) Population coherence and environmental impacts across spatial scales: a case study of Chinook salmon. Ecosphere 7: e01333

Oppel S, Hilton G, Ratcliffe N, Fenton C and others (2014) Assessing population viability while accounting for demographic and environmental uncertainty. Ecology 95: 1809–1818

Oppel S, Clark BL, Risi MM, Horswill C and others (2022) Cryptic population decrease due to invasive species predation in a long-lived seabird supports need for eradication. J Appl Ecol 59:2059–2070

Pacifici M, Foden WB, Visconti P, Watson JEM and others (2015) Assessing species vulnerability to climate change. Nat Clim Change 5:215–224

Payo-Payo A, Genovart M, Bertolero A, Pradel R, Oro D (2016) Consecutive cohort effects driven by density-dependence and climate influence early-life survival in a long-lived bird. Proc R Soc B 283:20153042

Pirotta E, Thomas L, Costa DP, Hall AJ and others (2022) Understanding the combined effects of multiple stressors: a new perspective on a longstanding challenge. Sci Total Environ 821:153322

Pitcher KW, Calkins DG (1981) Reproductive biology of Steller sea lions in the Gulf of Alaska. J Mammal 62: 599–605

Pitcher KW, Burkanov VN, Calkins DG, Le Boeuf BJ, Mamaev EG, Merrick RL, Pendleton GW (2001) Spatial and temporal variation in the timing of births of Steller sea lions. J Mammal 82:1047–1053

Plummer M, Best N, Cowles K, Vines K (2006) CODA: convergence diagnosis and output analysis for MCMC. R News 6:7–11 https://journal.r-project.org/archive/

Poloczanska ES, Burrows MT, Brown CJ, García Molinos J and others (2016) Responses of marine organisms to climate change across oceans. Front Mar Sci 3:62

Pradel R (2005) Multievent: an extension of multistate capture–recapture models to uncertain states. Biometrics 61:442–447

R Core Team (2022) R: a language and environment for statistical computing. R Foundation for Statistical Computing, Vienna. www.R-project.org

Rand K, McDermott S, Logerwell E, Matta ME and others (2019) Higher aggregation of key prey species associated with diet and abundance of the Steller sea lion *Eumetopias jubatus* across the Aleutian Islands. Mar Coast Fish 11:472–486

Raum-Suryan KL, Pitcher KW, Calkins DG, Sease JL, Loughlin TR (2002) Dispersal, rookery fidelity, and metapopulation structure of Steller sea lions (*Eumetopias jubatus*) in an increasing and a decreasing population in Alaska. Mar Mamm Sci 18:746–764

Regehr EV, Hostetter NJ, Wilson RR, Rode KD, Martin MS, Converse SJ (2018) Integrated population modeling provides the first empirical estimates of vital rates and abundance for polar bears in the Chukchi Sea. Sci Rep 8: 16780

Rhodes JR, Ng CF, de Villiers DL, Preece HJ, McAlpine CA, Possingham HP (2011) Using integrated population modelling to quantify the implications of multiple threatening processes for a rapidly declining population. Biol Conserv 144:1081–1088

Runge MC, Langtimm CA, Kendall WL (2004) A stage-based model of manatee population dynamics. Mar Mamm Sci 20:361–385

Santidrian Tomillo P, Robinson NJ, Sanz-Aguilar A, Spotila JR, Paladino FV, Tavecchia G (2017) High and variable mortality of leatherback turtles reveal possible anthropogenic impacts. Ecology 98:2170–2179

Saunders SP, Cuthbert FJ, Zipkin EF (2018) Evaluating population viability and efficacy of conservation management using integrated population models. J Appl Ecol 55:1380–1392

Schaub M, Gimenez O, Sierro A, Arlettaz R (2007) Use of integrated modeling to enhance estimates of population dynamics obtained from limited data. Conserv Biol 21: 945–955

Simpson D, Rue H, Riebler A, Martins TG, Sørbye SH (2017) Penalising model component complexity: a principled, practical approach to constructing priors. Stat Sci 32: 1–28

Sinclair EH, Zeppelin TK (2002) Seasonal and spatial differences in diet in the western stock of Steller sea lions (*Eumetopias jubatus*). J Mammal 83:973–990

Sinclair EH, Moore SE, Friday NA, Zeppelin TK, Waite JM (2005) Do patterns of Steller sea lion (*Eumetopias jubatus*) diet, population trend and cetacean occurrence reflect oceanographic domains from the Alaska Peninsula to the central Aleutian Islands? Fish Oceanogr 14: 223–242

Speckman PL, Sun D (2003) Fully Bayesian spline smoothing and intrinsic autoregressive priors. Biometrika 90: 289–302

Stabeno PJ, Schumacher JD, Ohtani K (1999) The physical oceanography of the Bering Sea. In: Loughlin TR, Ohtani K (eds) Dynamics of the Bering Sea. AK–SG–99–03. University of Alaska Sea Grant, Fairbanks, AK, p 1–28

Suryan RM, Arimitsu ML, Coletti HA, Hopcroft RR and others (2021) Ecosystem response persists after a prolonged marine heatwave. Sci Rep 11:6235

Sweeney KL, Birkemeier B, Luxa K, Gelatt T (2022) Results of Steller sea lion surveys in Alaska, June-July 2021. Memorandum to The Record, Feb 7, 2022. https://media.fisheries.noaa.gov/2022-02/ssl_aerial_survey_2021_final.pdf

Tavecchia G, Besbeas P, Coulson T, Morgan BJT, Clutton-Brock TH (2009) Estimating population size and hidden demographic parameters with state-space modeling. Am Nat 173:722–733

Tavecchia G, Sanz-Aguilar A, Cannell B (2016) Modelling survival and breeding dispersal to unobservable nest sites. Wildl Res 43:411–417

Taylor BL, Martinez M, Gerrodette T, Barlow J, Hrovat YN (2007) Lessons from monitoring trends in abundance of marine mammals. Mar Mamm Sci 23: 157–175

van Erp S, Oberski DL, Mulder J (2019) Shrinkage priors for Bayesian penalized regression. J Math Psychol 89: 31–50

Warlick AJ, Johnson DS, Gelatt TS, Converse SJ (2022) Environmental drivers of demography and potential factors limiting the recovery of an endangered marine top predator. Ecosphere 13:e4325

Warlick AJ, Himes Boor GK, McGuire TL, Shelden KEW and others (2023) Demographic and environmental drivers of population dynamics and viability in an endangered top predator using an integrated model. Anim Conserv. doi:10.1111/acv.12905

Winship AJ, Trites AW (2006) Risk of extirpation of Steller sea lions in the Gulf of Alaska and Aleutian Islands: a population viability analysis based on alternative hypotheses for why sea lions declined in Western Alaska. Mar Mamm Sci 22:124–155

York AE (1994) The population dynamics of Northern sea lions, 1975-1985. Mar Mamm Sci 10:38–51

York AE, Merrick RL, Loughlin TR (1996) An analysis of the Steller sea lion metapopulation in Alaska. In: McCullough DR (ed) Metapopulations and wildlife conservation. Island Press, Covelo, CA, p 259–292

Zhao Q, Boomer GS, Royle JA (2019) Integrated modeling predicts shifts in waterbird population dynamics under climate change. Ecography 42:1470–1481

Editorial responsibility: Clive McMahon, Hobart, Tasmania, Australia
Reviewed by: F. Medrano and 2 anonymous referees

Submitted: March 28, 2023
Accepted: September 27, 2023
Proofs received from author(s): December 2, 2023